DOI: 10.1002/ejic.200700004

Bis-μ-pyrazolate-Bridged Dinickel(II) and Dicopper(II) Complexes: An Example of Stereoelectronic Preference of Metal Ions and Stabilization of Mixed-Valence $Ni^{III}Ni^{II}$ Species

Vibha Mishra,[a] Francesc Lloret,[b] and Rabindranath Mukherjee*[a]

Keywords: Nickel / Copper / Dinuclear complexes / Pyrazolate bridge / Ni^{III}-Ni^{II} species

New dimeric nickel(II) and copper(II) complexes $[(L)Ni(\mu\text{-}L')]_2[ClO_4]_2$ **1** and $[(L)Cu(\mu\text{-}L')]_2[ClO_4]_2$ **2**, [2-[3-(2′-pyridyl)-pyrazol-1-ylmethyl]pyridine (L) and 3-(2-pyridyl)pyrazole (HL′)] have been synthesized, structurally characterized, and their absorption, magnetic, EPR and redox properties investigated. The crystal structure of **1**·MeCN reveals a planar $\{Ni_2(\mu\text{-}L')_2\}^{2+}$ core [Ni···Ni separation: 4.0765(10) Å] in which each distorted octahedral Ni^{II} ions is terminally coordinated by a tridentate ligand L and bridged by two HL′ units, in their deprotonated form. The structural analysis of **2**·2MeCN reveals two five-coordinate Cu^{II} ions, each terminally coordinated by adopting only a bidentate coordination mode of L, in which the $-CH_2$py arm remains uncoordinated. A similar bridging [Cu···Cu separation: 3.9382(24) Å] as in **1**·MeCN is observed. Thus stereoelectronic preferences of Ni^{II} and Cu^{II} are clearly revealed. Closer inspection of crystal packing diagram of **1**·MeCN reveals the formation of 2-D network structure assembled solely via C–H···π interaction [pyridyl C–H (4-position) of pyridylpyrazole unit of L and π cloud of pyridine of bridging deprotonated L′ unit]. In **2**·2MeCN, however, π···π interactions between uncoordinated pyridyl arms are observed. Variable-temperature magnetic studies on both complexes indicate the existence of strong antiferromagnetic coupling between the two metal ions (singlet-triplet energy separation, $J = -20\ cm^{-1}$ for **1** and $-200\ cm^{-1}$ for **2**). When investigated by cyclic voltammetry complex **1** displays two quasi-reversible electron-transfer reactions at $E_{1/2}$ = 1.36 V (ΔE_p = 110 mV) and 1.79 V (ΔE_p = 120 mV) vs. SCE, due to $Ni^{III}Ni^{II}/Ni^{II}{}_2$ and $Ni^{III}{}_2/Ni^{III}Ni^{II}$ redox processes, respectively. Constant potential electrolysis at 1.50 V vs. SCE leads to the generation of dark green mixed-valence $Ni^{III}Ni^{II}$ species, which is stable enough to be subjected to characterization by UV/Vis and EPR spectroscopy. Compound **2** exhibits only irreversible reductions (cathodic peak potential, E_{pc} = –0.28 V and –0.50 V vs. SCE).

Introduction

There has been continuing interest in the investigation of the magneto-structural properties of symmetrical dibridged metal(II) dimers.[1] As part of our continued involvement in the exploration of interesting coordination chemistry of pyridyl/pyrazole-based chelating ligands,[2] we have investigated the magneto-structural properties of a large variety of dinuclear/trinuclear/polymeric complexes with a varied combinations of endogenous/exogenous and solely exogenous bridging ligands (alkoxo/pyrazolato,[3] acetato/pyrazolato,[4] carbonato,[5] diacetato,[4,6] dichloro,[7] dihydroxo,[4,8] monohydroxo,[9] oxo/bis-acetato,[10,11] phenoxo/chloro,[12] phenoxo/hydroxo,[8,13] diphenoxo[14]).

Among the diverse bridging ligands/ligand frameworks that have been employed in holding two metal centers for efficient mediation of magnetic exchange interactions, pyrazolates are extensively explored, due to their coordination flexibility, versatility and potential to fine-tune metal–metal distance over a wide range of 2.4–4.6 Å affording oligo- and polymetallic compounds.[15]

This work finds impetus from the fact that a combination of carefully designed chelating ligands and judicious choice of metal ions with stereoelectronic preference can lead to the synthesis of metal complexes with interesting molecular and electronic structural properties.[16,17] The choice of terminal ligands of this work stems from our continued activity in the coordination chemistry of nonplanar pyridyl/pyrazole ligands toward transition metal ions.[2,4,6,7,18,19] Specifically, in the present work our target has been to synthesize and structurally characterize dimetal(II) complexes, satisfying the following requirements. (i) The metal ions should show stereoelectronic preference in their coordination. (ii) The terminal coordination of the metal ions should be provided by tridentate ligand L and bridging coordination by deprotonated form of 3-(2-pyridyl)pyrazole

[a] Department of Chemistry, Indian Institute of Technology Kanpur,
Kanpur 208 016, India
Fax: +91-2597436
E-mail: rnm@iitk.ac.in
[b] Departament de Química Inorgànica/Instituto de Ciencia Molecular (ICMOL),
Facultat de Química de la Universitat de València,
Dr Moliner, 46100 Burjassot (València), Spain

Supporting information for this article is available on the WWW under http://www.eurjic.org or from the author.

(HL′).[16,17,20] (iii) The magneto-structural behavior should be investigated. Thus we report here the synthesis, crystal structure of bis-μ-pyrazolate-bridged dimetal(II) complexes $[(L)M^{II}(\mu\text{-}L')]_2[ClO_4]_2$ (M = Ni **1**, Cu **2**), and investigation of their spectroscopic, magnetic, and redox properties.

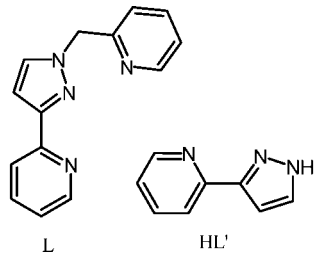

Results and Discussion

Synthesis and General Characterization

The designed synthesis of two complexes $[\{(L)M^{II}(\mu\text{-}L')\}_2][ClO_4]_2$ (M = Ni **1**, Cu **2**) are based on the following considerations: (i) L is a potential tridentate ligand,[18d] (ii) 3-(2-pyridyl)pyrazole (HL′)[20] can assume several coordination modes and the one adopted in the complex formation is governed by the reaction conditions.[21] Notably, it can act as a terdentate bridging ligand via deprotonation of the pyrazolyl NH group and coordination of the pyrazolyl N atom to a second metal ion, and (iii) The Cu^{II} ion is well-known to produce variable and distorted coordination geometries[22] and the Ni^{II} ion is expected to produce six-coordinate geometry with the given combination of ligands L and deprotonated L′. Keeping these points in mind a common synthetic strategy was followed for preparing the two complexes. The metal salt $Ni(OAc)_2{\cdot}4H_2O$/$[Cu(H_2O)_6][ClO_4]_2$ and L (1:1) were allowed initially to react in MeOH, addition of 1 equiv. of HL′, followed by addition of Et_3N led to the formation/isolation of the complexes.

As expected, both complexes behave as 1:2 electrolytes in MeCN solution.[23] IR spectra show the characteristic bands at ca. 1100 cm^{-1} and ca. 620 cm^{-1} for ionic perchlorate vibrations. Elemental analysis, IR, and solution electrical conductivity data are in excellent agreement with the above formulations of the two new complexes.

Crystal Structure of $[\{(L)Ni(\mu\text{-}L')\}_2][ClO_4]_2$ (1·MeCN)

A perspective view of the cation of **1**·MeCN with atom numbering scheme is shown in Figure 1 and selected metric parameters are given in Table 1. Each Ni^{II} ion is in six-coordinate geometry with coordination by two bridging pyrazolate nitrogen atoms [N(6) and N(14) to Ni1; N(7) and N(13) to Ni2], a terminal pyridyl coordination from 3-(2-pyridyl)pyrazole units N(5) to Ni1 and N(12) to Ni2. Two additional coordinations are achieved by pyrazole nitrogen of ligand L: N(2) to Ni1 and N(9) to Ni2. Two long axial coordinations are achieved by the pyridyl nitrogen atoms of L: N(1) and N(4) for Ni1; N(8) and N(11) for Ni2. Both Ni^{II} ions are bridged by the deprotonated 3-(2-pyridyl)pyrazole unit, leading to a Ni···Ni separation of 4.0765(10) Å. In essence, it is a bis(μ-pyrazolate)-bridged six-coordinate dinickel(II) complex. Metric parameters indicate that the coordination geometry deviates from regular octahedron. While the *trans* angles vary in the range 160–175° the *cis* angle variation is in the range 77–101° (Table 1).

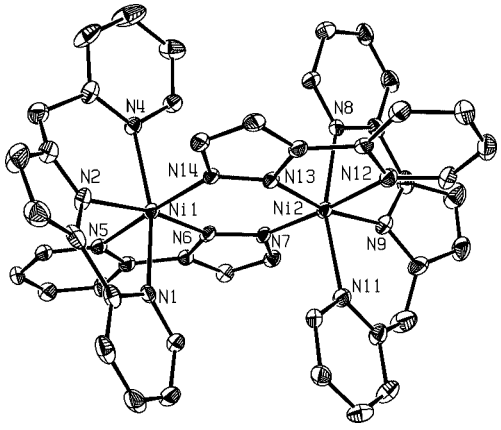

Figure 1. View of the dication $[(L)_2Ni_2(\mu\text{-}L')_2]^{2+}$ in complex **1**·MeCN, showing the atom numbering scheme. Atoms are drawn at 30% probability level. All hydrogen atoms are excluded for clarity.

The two nickel(II) ions deviate from the mean plane passing through bridging pyrazolate units by only 0.1482 Å and 0.0765 Å (Ni1 and Ni2, respectively). Dihedral angle between the plane of pyrazolate ring of {Ni1(μ-L′)} unit and {Ni2(μ-L′)} is 5.529(172)°. In this structure there are three types of donor atoms: pyrazole nitrogen and two types of pyridyl nitrogen atoms. Average distances for Ni–N_{py} (directly attached pyridyl ring), Ni–N_{py} (pyridyl ring with CH_2-spacer), and Ni–N_{pz} (pyrazole ring) are 2.1575(4), 2.173(4) and 2.0333(4) Å, respectively. It is found that pyrazole rings from terminal ligands are more strongly bonded to the Ni^{II} ions than the bridging ones. In fact, the observed Ni–N_{py} (N5/N12) (bridging pyrazolate) distances are shorter than Ni–N_{py} (N1/N8) bond lengths from terminally coordinated L ligand [2.128(4) and 2.152(4) Å vs. 2.160(4) and 2.189(4) Å]. The present complex is amongst relatively few structurally characterized bis(μ-pyrazolate)-bridged dinickel(II) complexes.[2a,24,25]

Crystal Structure of $[\{(L)Cu(\mu\text{-}L')\}_2][ClO_4]_2{\cdot}2MeCN$ (2·2MeCN)

A perspective view of the cation of **2**·2MeCN is displayed in Figure 2, along with the atom-numbering scheme. The structural analysis reveals that crystallographic asymmetric unit consists of a binuclear dipyrazolate-bridged copper(II) cation, two perchlorate ions, and two MeCN molecules. The dication sits on a crystallographically imposed inversion center and hence only half of the dimeric unit is unique and the other half is symmetry-related. Each Cu^{II} ion is in five-coordinate geometry with coordination by two bridging pyrazolate nitrogen atoms [N(6) and N(7) for Cu1;

Table 1. Selected bond lengths [Å] and angles [°] of **1**·MeCN and **2**·2MeCN.

1·MeCN		**2**·2MeCN	
Ni(1)–N(1)	2.160(4)	Cu(1)–N(1)	2.040(6)
Ni(1)–N(2)	2.014(4)	Cu(1)–N(2)	2.302(7)
Ni(1)–N(4)	2.178(4)	Cu(1)–N(5)	2.054(6)
Ni(1)–N(5)	2.128(4)	Cu(1)–N(6)	1.940(6)
Ni(1)–N(6)	2.033(3)	Cu(1)–N(7)^{i}	1.971(6)
Ni(1)–N(14)	2.064(4)		
Ni(2)–N(7)	2.037(4)		
Ni(2)–N(8)	2.189(4)		
Ni(2)–N(9)	2.017(4)		
Ni(2)–N(11)	2.168(4)		
Ni(2)–N(12)	2.152(4)		
Ni(2)–N(13)	2.035(3)		
N(1)–Ni(1)–N(2)	77.16(15)	N(2)–Cu(1)–N(1)	76.5(2)
N(1)–Ni(1)–N(4)	162.53(14)	N(2)–Cu(1)–N(5)	91.9(2)
N(1)–Ni(1)–N(5)	89.26(13)	N(2)–Cu(1)–N(6)	108.8(2)
N(1)–Ni(1)–N(6)	97.80(14)	N(2)–Cu(1)–N(7)^{i}	96.1(2)
N(1)–Ni(1)–N(14)	91.58(14)	N(1)–Cu(1)–N(5)	90.7(2)
N(2)–Ni(1)–N(4)	85.38(15)	N(1)–Cu(1)–N(6)	169.8(2)
N(2)–Ni(1)–N(5)	92.11(15)	N(1)–Cu(1)–N(7)^{i}	89.9(2)
N(2)–Ni(1)–N(6)	169.96(16)	N(5)–Cu(1)–N(6)	80.6(3)
N(2)–Ni(1)–N(14)	92.47(15)	N(5)–Cu(1)–N(7)^{i}	171.9(3)
N(4)–Ni(1)–N(5)	91.92(14)	N(6)–Cu(1)–N(7)^{i}	98.0(2)
N(4)–Ni(1)–N(6)	99.54(14)		
N(4)–Ni(1)–N(14)	88.62(14)		
N(5)–Ni(1)–N(6)	79.04(14)		
N(5)–Ni(1)–N(14)	175.42(14)		
N(6)–Ni(1)–N(14)	96.38(14)		
N(7)–Ni(2)–N(8)	96.22(14)		
N(7)–Ni(2)–N(9)	93.04(15)		
N(7)–Ni(2)–N(11)	92.87(15)		
N(7)–Ni(2)–N(12)	175.12(14)		
N(7)–Ni(2)–N(13)	96.42(14)		
N(8)–Ni(2)–N(9)	77.66(15)		
N(8)–Ni(2)–N(11)	160.88(14)		
N(8)–Ni(2)–N(12)	83.01(14)		
N(8)–Ni(2)–N(13)	94.52(14)		
N(9)–Ni(2)–N(11)	85.11(15)		
N(9)–Ni(2)–N(12)	91.50(15)		
N(9)–Ni(2)–N(13)	168.34(16)		
N(11)–Ni(2)–N(12)	89.29(15)		
N(11)–Ni(2)–N(13)	101.16(14)		
N(12)–Ni(2)–N(13)	78.86(15)		

Symmetry code: (i) = $-x + 2, -y + 1, -z + 1$

N(6′) and N(7′) for Cu1′], a terminal pyridyl coordination N(5)/N(5′) from 3-(2-pyridyl)pyrazole units, and a pyridyl nitrogen atom N(1)/N(1′) from the ligand L in the equatorial plane. Axial coordination is achieved by the pyrazole nitrogen atom [Cu–N(2): 2.302(7) Å] of ligand L. A noteworthy feature of this structure is that in each ligand L the methyl pyridine arm remains uncoordinated. Thus the Cu^{II} center has square-pyramidal geometry [precisely it is slightly distorted ($\tau = 0.035$)],[26] which is achieved by having the two potentially tridentate chelating units of L acting as bidentate ligands. The preference of the Cu^{II} ion for five-coordination over six, is a consequence of Jahn–Teller distortion.[18c] The Cu(1) atom lies above the equatorial plane by 0.118 Å towards pyrazole nitrogen N(2) of terminally coordinated L. The sum of four angles provided by the equatorial nitrogen donors is 359.2°, consistent with a small displacement of the copper atom from the equatorial plane. The two Cu^{II} ions are bridged by the deprotonated 3-(2-pyridyl)pyrazole unit, leading to a Cu···Cu separation of 3.9382(24) Å. In essence, it is a bis(μ-pyrazolate)-bridged dicopper(II) complex in which a planar $\{Cu_2(\mu\text{-}L')_2\}^{2+}$ core is terminally coordinated by two L ligands, in which methyl-pyridine arms remain uncoordinated. The Cu···Cu distance is on the higher end of distances reported for complexes with similar structural motif.[2,21,27–29]

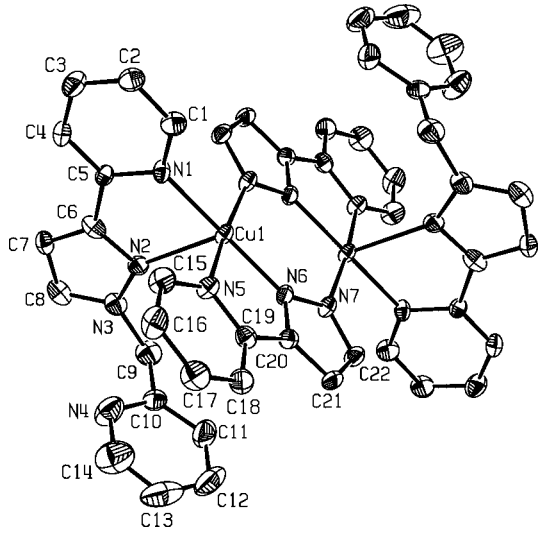

Figure 2. View of the dication $[(L)_2Cu_2(\mu\text{-}L')_2]^{2+}$ in complex **2**·2MeCN, showing the atom numbering scheme. Atoms are drawn at 30% probability level. All hydrogen atoms are excluded for clarity.

Noncovalent Interactions

A closer inspection of the crystal packing diagram of **1**·MeCN reveals that the cations are engaged in an extensive intermolecular C–H···π interactions[18f,30a,30b] involving *para*-C–H of coordinating pyridine ring of pyridylpyrazole unit of L with the π-electron cloud of pyridine ring of bridging 3-(2-pyridylpyrazole) unit. Interaction parameters are given in Table 2. These C–H···π interactions led to the formation of linear one-dimensional chains (Figure 3, a). These chains are interconnected via neighboring molecules of adjacent chain through another C–H···π interaction involving *para*-C–H of pyridine ring of bridging 3-(2-pyridyl)pyrazole unit with the π-electron cloud of coordinating pyridine ring of pyridylpyrazole unit of L. This resulted in the formation of 2D network (Figure 3, b). This is rather interesting that

Table 2. Hydrogen-bonding (C–H···π) parameters for $[(L)_2Ni_2(\mu\text{-}L')_2]^{2+}$ in **1**·MeCN.

D–H···π	H···π /Å	*D*···π /Å	*D*–H···π
C3–H3···Ct1	2.4737^{i}	3.47866(3)^{i}	173.2°^{i}
C16–H16···Ct2	2.7767^{ii}	3.6668(3)^{ii}	147.4°^{ii}
C25–H25···Ct3	2.5490^{iii}	3.5127(3)^{iii}	159.96°^{iii}

(i) $-x, 1-y, 1-z$; (ii) $-x, 1-y, -z$; (iii) $-x, -y, 2-z$

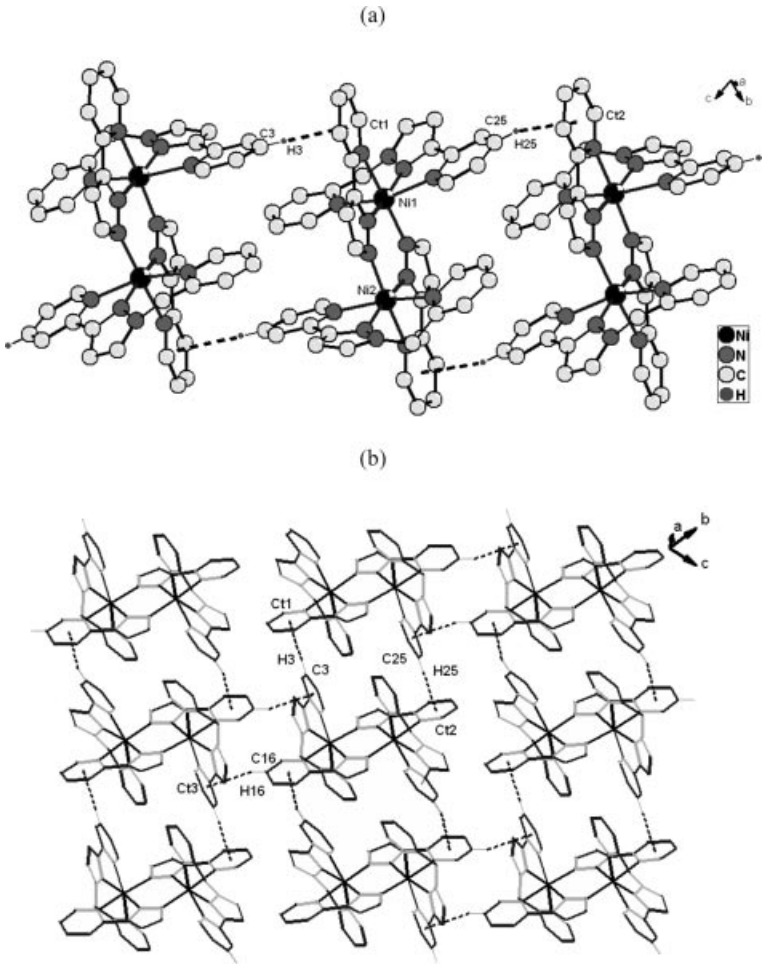

Figure 3. (a) A perspective view of the formation of a linear chain and (b) Formation of 2D-network solely via C–H···π interactions in the dication $[(L)_2Ni_2(\mu\text{-}L')_2]^{2+}$ of complex **1**·MeCN. All hydrogen atoms except those involved in hydrogen-bonding are excluded for clarity.

such 2D architecture has formed solely via C–H···π interactions.

The molecular packing in the crystal structure of **2**·2MeCN does not reveal C–H···π interactions, as observed for **1**·MeCN. However, it is realized that uncoordinated pyridine arm of L is involved in intermolecular π-π stacking,[19a,30c] leading to the formation of staircase-like arrangement of molecules (see Figure S1 in the electronic Supporting Information). The π···π stacking parameters are as follows: centroid–centroid distance: 3.9570(17) Å; perpendicular distance between two CH_2-py arm: 3.5682 Å; dihedral angle between the planes is 0.0°; displacement angle β = 25.60°.[18f,30] The difference in the nature of noncovalent interactions observed for **1**·MeCN and **2**·2MeCN must have originated from dissimilar nature of metal coordination mode of ligand L. While for the former complex the potential tridentate ligand L acts as a tridentate ligand in the case of the latter complex it acts as a bidentate ligand leaving the CH_2py arm uncoordinated. This effect caused by stereoelectronic geometric preference of metal ions is manifested in the observed noncovalent interactions for these two structures.

We present here a rationalization of observed secondary interactions. C–H···π interactions observed in **1**·MeCN is facilitated due to *meridional* coordination of L which forces the ligand L to attain planar and perpendicular orientation to the bridging 3-(2-pyridylpyrazole) unit (Figure 1). Hence we believe that the relative disposition of L and bridging 3-(2-pyridylpyrazole) unit in **1**·MeCN favors the formation of 2D network via extensive C–H···π interactions. Such a situation is absent in **2**·2MeCN due to uncoordinated CH_2-py arm of L (Figure 2) and therefore C–H···π interaction is not observed in **2**·2MeCN. In **2**·2MeCN, however, the uncoordinated CH_2-py arms are suitably placed away from the metal center and remains almost parallel to the pyridine ring of the bridging 3-(2-pyridylpyrazole) unit. This in turn triggers to engage in weak intermolecular π-π stacking interactions (Figure S1) involving CH_2-py arm of L.

Absorption Spectra

Absorption spectra for both complexes in MeCN are displayed in Figure S2. Purplish-green solutions of complex **1**

exhibit crystal-field transitions at 966 nm and 526 nm, which could be assigned as $^3A_{2g}\rightarrow{}^3T_{2g}$ and $^3A_{2g}\rightarrow{}^3T_{1g}$ (in octahedral coordination environment), respectively. A spin forbidden transition could be identified at 800 nm ($^3A_{2g}\rightarrow{}^1E_g$).[31] Compound **2** exhibits a crystal-field transition at 640 nm with a shoulder at 850 nm, typical of square-pyramidal Cu^{II} stereochemistry.[22] An intense transition occurs as a shoulder at ca. 300 nm probably due to pyrazolate $\rightarrow Cu^{II}$ charge-transfer. Absorptions at higher energy originate in the intraligand.

Magnetic Properties

Complexes **1** and **2** have the same planar $[M^{II}(\mu\text{-}L')]_2$ (M = Ni and Cu) binuclear entities, with the Ni^{II} ion having distorted octahedral and Cu^{II} ion assuming square-pyramidal geometry. From the magnetic point of view these complexes are clearly of interest and give us a unique opportunity to compare their magnetostructural behavior. The magnetic behavior of **1** (Figure 4) deserves special attention owing to the status of this complex as one among very few examples of bis(μ-pyrazolate)-bridged Ni^{II} dimers.[2a,24,25] The temperature-dependence of the magnetic behavior is shown in Figure 4 in the form of $\chi_M T$ and χ_M vs. T plots. The observed $\chi_M T$ value of 2.16 $cm^3 mol^{-1} K$ (2.94 μ_B/Ni) at room temperature is indicative of $S = 1$ system. The value of $\chi_M T$ decreases very smoothly when cooling and it is 1.87 $cm^3 mol^{-1} K$ at 100 K (2.73 μ_B/Ni). Below this temperature $\chi_M T$ decreases rapidly and it vanishes when T tends to zero. The χ_M curve shows a maximum at 30 K. It clearly reveals the presence of antiferromagnetically coupled Ni^{II} ions in **1**. According to the dinuclear nature of the complex, the experimental data were modeled through the Hamiltonian $H = -J\hat{S}_1\hat{S}_2 + D(\hat{S}_{z1}^2 + \hat{S}_{z2}^2)$ (with $\hat{S}_1 = \hat{S}_2 = 1$)[32] in the range from 298 K to 2.1 K. In this case, the magnetic susceptibility for a Ni^{II} dimer is given by Equation (1).

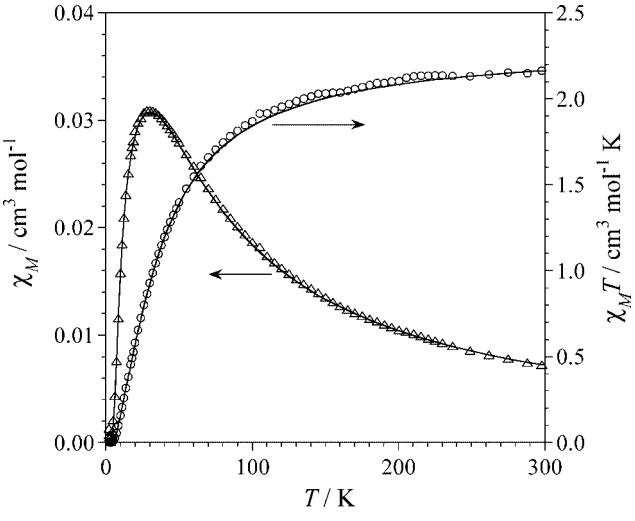

Figure 4. Temperature-dependence of the χ_M and $\chi_M T$ product for powdered sample of $[(L)_2Ni_2(\mu\text{-}L')_2][ClO_4]_2$ (**1**). The solid lines represent the best theoretical fit using the equation described in the text.

$$\chi_M = \frac{2N\beta^2 g^2}{3\alpha}\left(\frac{F_1}{kT} + \frac{2F_2}{D} + \frac{6a^2F_3}{3J-\Delta} + \frac{6b^2F_4}{3J+\Delta}\right)$$

$$F_1 = 1 + \exp(2x) + 4\exp(2x+y)$$

$$F_2 = -1 + 2\exp(2x+y) + \exp(y) - 2\exp(2x)$$

$$F_3 = \exp(2x) - \exp(\frac{x}{2} + z)$$

$$F_4 = \exp(2x) - \exp(\frac{x}{2} - z)$$

$$\alpha = 2 + \exp(y) + \exp(\frac{x}{2} - z) + \exp(\frac{x}{2} + z) + \ldots$$
$$\ldots\ 2\exp(2x) + 2\exp(2x+y)$$

$$x = \frac{J}{kT};\quad y = \frac{D}{kT};\quad z = \frac{\Delta}{kT};\quad \Delta = \left[(3J+D)^2 - 8JD\right]^{1/2}$$

$$a = \frac{9J - D + 3\Delta}{\left[(9J - D + 3\Delta)^2 + 8D^2\right]^{1/2}}$$

$$b = \frac{2\sqrt{2D}}{\left[(9J - D + 3\Delta)^2 + 8D^2\right]^{1/2}} \qquad (1)$$

To reduce the number of variables the D (zero-field splitting parameter) and g values were considered to be identical for the two nickel(II) ions. A satisfactory fit was obtained with the set of parameters $J = -20.6\ cm^{-1}$, $|D| = 1.2\ cm^{-1}$ and $g = 2.15$ [$R = 1.3\times10^{-5}$, $R = \Sigma(\chi_M{}^{obs} - \chi|_M{}^{calc})^2/\Sigma(\chi_M{}^{obs})^2$], confirming the intramolecular antiferromagnetic coupling between nickel(II) centers. The temperature-independent paramagnetism, TIP, was observed to be 90 $cm^3 mol^{-1}$ for each Ni^{II} ion, which was corrected on the magnetic curve of Figure 4. No paramagnetic impurities were observed. The magnitude of the exchange interaction is comparable to that observed for closely similar compounds.[25]

Generally, the dicopper(II) complexes with pyrazolate-bridge show a very strong antiferromagnetic coupling.[2,21,27–29] Variable-temperature (5–300 K) magnetic studies were done on powdered samples in order to determine the magnitude of the magnetic coupling of **2**. In fact, compound **2** shows a subnormal magnetic moment at room temperature (μ_{eff}/Cu = 1.58 μ_B). The $\chi_M T$ value decreases gradually upon cooling and it reaches a plateau below 50 K. A plot of $\chi_M T$ vs. T for **2** (Figure 5) is typical of a moderate antiferromagnetically coupled dicopper(II) complex. The experimentally observed χ_M values (per dimer) were fitted to the modified[3,4,8b,9,12–14] Bleaney–Bowers equation based on the Heisenberg spin Hamiltonian, $H = -JS_1 \cdot S_2$ [Equation (2)], allowing for the presence of monomeric copper(II) impurity behaving as a Curie paramagnet, where ρ is the mole fraction of such an impurity and N_α is the temperature-independent paramagnetism per Cu^{II} ion; other symbols have their usual meaning. Keeping g and N_α fixed at 2.1 [obtained from the EPR spectrum of the complex, Figure S3 {typical value for a tetragonal Cu^{II}[4]}] and $60\times10^{-6}\ cm^3 mol^{-1}$, the J and ρ parameters

were determined by minimizing $R = \Sigma(\chi_M^{obs} - \chi_M^{calc})^2/\Sigma(\chi_M^{obs})^2$ using Equation (2) gave good data fits. As shown by the trace in Figure 5, an excellent simulation (non-linear regression analyses) of the data could be attained with the following parameters: $J = -200\ cm^{-1}$ and $\rho = 0.86\%$. $R = 1.84 \times 10^{-7}$ for **2**. The magnitude of the exchange interaction is similar to that observed for other bis(μ-pyrazolate)-bridged[28,29] and the related bis(μ-N^1,N^2)triazole-bridged[33] dinuclear Cu^{II} complexes. Solution-state μ_{eff}/Cu value for **2** at 298 K is 1.4 μ_B, slightly lower than that obtained as a solid.

$$\chi_M = 2N\beta^2g^2/3kT\,[1 + 1/3\exp(-J/kT)]^{-1}(1-\rho) + (N\beta^2g^2/2kT)\rho + 2N\alpha \quad (2)$$

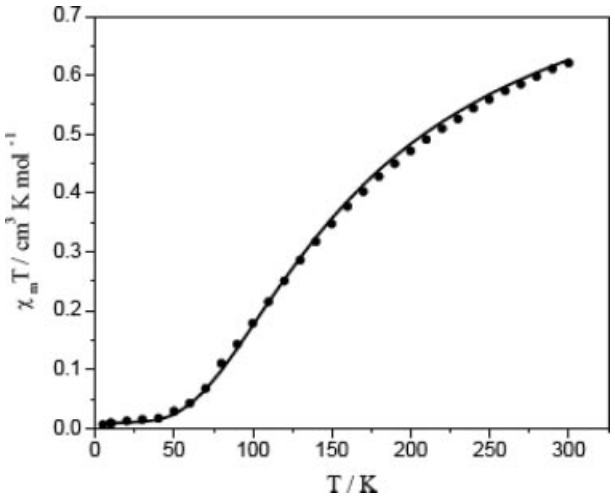

Figure 5. Temperature dependence of the $\chi_M T$ product for powdered samples of $[(L)_2Cu_2(\mu\text{-}L')]_2[ClO_4]_2$ (**2**). The solid lines represent the best theoretical fit using the equation described in the text.

In these complexes the pathway for magnetic exchange is propagated through the bridging pyrazolate ligands. From the molecular structure of **2**, one can conclude that the unpaired electron in each metal center is clearly described by $d_{x^2-y^2}$ magnetic orbital, which is coplanar with the pyrazolate skeleton (see part a of Scheme 1). The significant overlap between these magnetic orbitals accounts for the strong antiferromagnetic coupling observed.

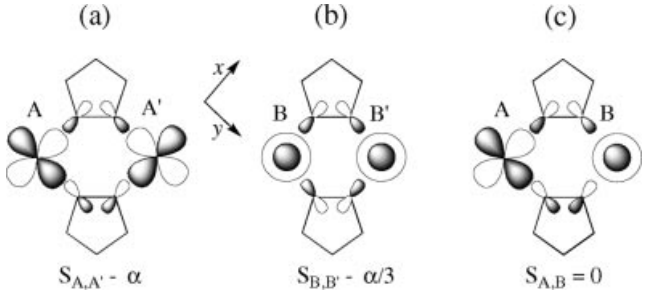

Scheme 1.

It is interesting to observe that the value of J for Ni^{II} dimer (ca. $-20\ cm^{-1}$) is much lower than the corresponding value for the Cu^{II} dimer (ca. $-200\ cm^{-1}$).[34] In **1**, the Ni^{II} ion has two magnetic orbitals, $d_{x^2-y^2}$ and d_{z^2} (see Scheme 1). In order to evaluate both magnetic exchange pathways, we can describe the unpaired electrons on each Ni^{II} ion by the orbitals Ψ_A and Ψ_B [Equations (3) and (4)], where &πηι;$_L$ is the orbital of the bridging ligand.[35] The participation of the peripheral ligands is neglected and the same energy for both metal orbitals was assumed (the same mixing coefficient a).

$$\Psi_A = N(d_{x^2-y^2} - a\phi_L) \quad (3)$$

$$\Psi_B = N(d_{z^2} - \frac{a}{\sqrt{3}}\ \phi_L) \quad (4)$$

In the frame of Kahn's orbital model[36] it is found that J varies as $S_{u,v}^2$ ($S_{u,v}$ being the overlap integral between the magnetic orbitals u and v). The values of $S_{u,v}$ can be approximated to be $S_{A,A'} = \langle\Psi_A|\Psi_{A'}\rangle \propto a^2$ and $S_{B,B'} = \langle\Psi_B|\Psi_{B'}\rangle \propto \frac{a^2}{3}$, where the prime refers to the second magnetic orbital in the dimer. In this approach, our prediction concerning the relative magnitudes of both pathways is $\frac{J_{x^2-y^2,x^2-y^2}}{J_{z^2,z^2}} \approx \frac{S_{A,A'}^2}{S_{B,B'}^2} \approx 9$, showing the greater magnetic exchange through the $d_{x^2-y^2}$ pathway.[35]

When the metal ion has more than one unpaired electron, the experimental J parameter must be decomposed into a sum of individual contributions, J_{uv}, concerning each pair of magnetic orbitals involved in the exchange phenomenon [Equation (5)], where n_A and n_B are the number of unpaired electrons associated with the transition metal ions A and B, respectively.[36,37] Equations (5), (6), and (7) show how the magnitude of the antiferromagnetic interaction is not properly described by J but by n_An_BJ. In the present case ca. $-80\ cm^{-1}$ for Ni^{II} ($n_A = n_B = 2$) respect to ca. $-200\ cm^{-1}$ for Cu^{II} dimer ($n_A = n_B = 1$), values which are still too different.

$$J = \frac{1}{n_An_B}\sum_{u=1}^{n_A}\sum_{v=1}^{n_B} J_{uv} \quad (5)$$

$$J_{CuCu} = J_{x^2-y^2,x^2-y^2} \approx -200\ cm^{-1} \quad (6)$$

$$J_{NiNi} = \frac{1}{4}(J_{x^2-y^2,x^2-y^2} + J_{z^2,z^2} + J_{x^2-y^2,z^2}) \approx -20\ cm^{-1} \quad (7)$$

The low value for the Ni^{II} dimer can be attributed to the existence of ferromagnetic terms between the magnetic orbitals $d_{x^2-y^2}$ and d_{z^2} (strict orthogonality, Scheme 1, c), which can be important when the distance between paramagnetic centers is short (cases of mono- and diatomic bridges).[38] Assuming a similar energy and bond lengths for Ni^{II} and Cu^{II} complexes and taking into account that $J_{x^2-y^2,x^2-y^2} \approx 9J_{z^2,z^2} \approx -200\ cm^{-1}$ (see above), a rough value of $J_{x^2-y^2,z^2} \approx +70\ cm^{-1}$ can be inferred from Equation (7), which is of the same order as that observed for diatomic bridges such as oximes.[37]

Redox Properties

The redox behavior of these complexes has been investigated by cyclic voltammetry (CV) in MeCN at a platinum electrode (scan rate 100 mV s^{-1}). Complex **1** exhibits both oxidative as well as reductive redox behavior. In the potential range 0.0 to 2.0 V it undergoes two one-electron quasi-reversible oxidations (Figure 6) at [$E_{1/2}$ = +1.36 V (ΔE_p = 110 mV)] and [$E_{1/2}$ = +1.79 V (ΔE_p = 120 mV) vs. SCE], respectively. The two processes are tentatively assigned to the formation of $Ni^{III}Ni^{II}$ and $Ni^{III}Ni^{III}$ species. During negative scan 0.0 to –2.0 V it exhibits an irreversible response at –1.52 V vs. SCE. Such oxidative redox behavior is similar to other dinickel(II) complexes reported in the literature.[39] Notably, the difference between the successive redox processes in **1** is sufficient (ca. 450 mV) to stabilize the mixed-valence $Ni^{III}Ni^{II}$ species. Controlled-potential electrolysis of **1** at an applied potential of +1.50 V vs. SCE in MeCN solution consumed $n = 0.95 \pm 0.02$ e$^-$/complex (mean value of three independent measurements) and produced dark green solutions. Such solutions display the same CV response as that of $Ni^{II}Ni^{II}$ species. However, this time the response at 1.36 V is reductive, as expected (Figure S4). Re-reduction of such solutions at 0.0 V caused a transfer of 85% of the charge that passed during oxidation, attesting reasonable stability of the oxidized mixed-valence $Ni^{III}Ni^{II}$ species. Absorption spectra of dark green solutions (Figure 7) display a characteristic broad band at 755 nm (ε = 930 M^{-1} cm^{-1}). No other absorption is noted. In more likelihood this has happened either due to superposition of the spectra of individual Ni^{II} and Ni^{III} ions or due to strong delocalization (X-ray structure of **1**·MeCN), properties of the component species have been replaced by a new delocalized species. However, the high molar extinction coefficient value than that expected for a d-d band indicates it to be an IVCT band. The dark green color of the oxidized solution is similar to those of similar Ni^{III}-Ni^{II} mixed-valence species reported in the literature.[40]

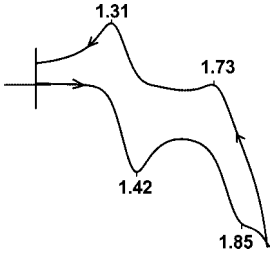

Figure 6. Cyclic voltammogram (100 mV s^{-1}) of [$(L)_2Ni_2$ (μ-L′)$_2$]-[ClO_4]$_2$ (**1**) at a Pt electrode in MeCN (ca. 0.1 dm^3 mol^{-1} in TBAP). Indicated potentials (in V) are vs. SCE.

To throw more light on the nature of this supposedly mixed-valence species the dark green solution has been further characterized by EPR spectral measurements. The EPR spectrum of coulometrically generated solutions recorded at 120 K is shown in Figure 8. The spectrum is characteristics of S = 3/2 system with g values 2.08, 3.20, and 5.29, arising out of spin-exchange coupling between S = 1 Ni^{II} state and S = 1/2 Ni^{III} state.[39] The Ni^{III} ion is considered to be low-spin since all known Ni^{III} complexes to date are low-spin.[41] To strengthen our hypothesis we measured solution-state magnetic susceptibility of the green solution. The μ_{eff} value of 4.33 μ_B at 293 K (Evans method),[42] for two independent measurements, confirm our claim that it is a S = 3/2 system.

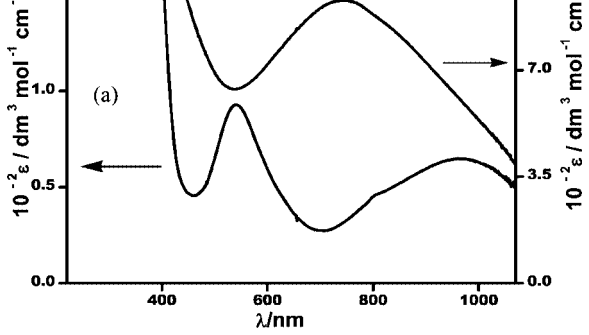

Figure 7. UV/Vis spectra in the range 400–1100 nm (in MeCN) of (a) [{$(L)_2Ni_2(\mu\text{-}L')$}$_2$][ClO_4]$_2$ (**1**) and (b) coulometrically oxidized green solution (1.67 mM) at 1.50 V vs. SCE.

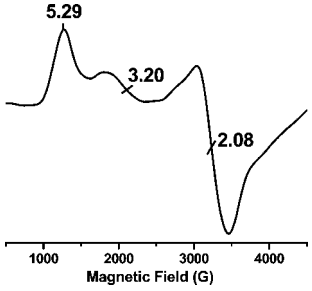

Figure 8. EPR spectrum at 120 K of coulometrically generated green solution of $[(L)_2Ni_2(\mu\text{-}L')_2]^{3+}$ in MeCN.

Dicopper(II) complex **2** displays two cathodic responses with E_{pc} values of –0.28 V and –0.50 V vs. SCE (Figure S5), due to $Cu^{II}{}_2$/$Cu^{II}Cu^{I}$ and $Cu^{II}Cu^{I}$/$Cu^{I}{}_2$ redox processes, respectively. On reversal scan, only one anodic response at 0.24 V vs. SCE was observed. This behavior is indicative of an unstable mixed-valence $Cu^{II}Cu^{I}$ and $Cu^{I}{}_2$ species. Given the planarity of the $\{Cu(\mu\text{-}L')\}_2{}^{2+}$ unit, this result is understandable, as Cu^{I} would prefer to assume tetrahedral geometry.

Concluding Remarks

In this report designed synthesis of bis(μ-pyrazolate)-bridged dinickel(II) and dicopper(II) complexes has been achieved with a simple potentially tridentate ligand L and bridging ligand 3-(2-pyridyl)pyrazole. Structural proof for the complexes illustrates a neat example of stereoelectronic geometric requirement of M^{II} ion: Ni^{II} preferring six- and Cu^{II} preferring five-coordination. The outcome of stereoelectronic preference is manifested in the observed noncovalent interactions: C–H···π in the case of **1**·MeCN and

π···π for **2**·MeCN, dictated by the spatial disposition of L around M^{II} ion. Temperature-dependent magnetic studies reveal the presence of antiferromagnetic coupling in both, the extent of coupling is more in the case Cu^{II} dimer than in the case of Ni^{II} dimer. Generation and stabilization of mixed-valence Ni^{III}-Ni^{II} species presented in this work encourage the synthesis of other variety of pyrazolate-bridged nickel(II) complexes in order to gain a better understanding of redox chemistry of dinickel(II) systems.

Experimental Section

General: All chemicals were obtained from commercial sources and used as received. Solvents were purified/dried following standard procedures.[3–14] The ligand L was prepared as before.[18d] 3-(2-pyridyl)pyrazole (HL′) was synthesized following a reported procedure.[20] Tetra-*n*-butylammonium perchlorate (TBAP), was prepared/purified as before.[11]

Syntheses

Preparation of [{(L)Ni(μ-L′)}$_2$][ClO$_4$]$_2$ (1): To a stirred solution of $Ni(OAc)_2{\cdot}4H_2O$ (0.052 g, 0.212 mmol) in MeOH (3 cm^3), L (0.050 g, 0.212 mmol) was added in small portions. After stirring for 30 min, HL′ (0.031 g, 0.212 mmol) was added and the resulting mixture was stirred for 5 min, followed by addition of Et_3N (0.021 g, 0.212 mmol). The reaction mixture was then allowed to stir for a further 30 min. Solid sodium perchlorate (0.052 g, 0.424 mmol) was added to it and the mixture was kept in air for slow evaporation, which led to the precipitation of a purple microcrystalline solid. It was filtered, washed with MeOH and dried in vacuo (yield: 0.052 g, ca. 45%). $C_{44}H_{36}Cl_2N_{14}Ni_2O_8$ (1077.98): calcd. C 49.02, H 3.36, N 18.19%; found C 48.95, H 3.41, N 17.83%. Molar conductance, Λ_M (MeCN, 298 K) = 240 Ω^{-1}cm^{2}mol^{-1} (expected range[23] for 1:2 electrolytes: 220–300 Ω^{-1}cm^{2}mol^{-1}). UV/Vis (MeCN), λ_{max}/nm (ε/M^{-1}cm^{-1}): 966 (65), 800 (sh) (48), 526 (93), 315 (sh) (20 000), 290 (sh) (33 200), 254 (44 729). μ_{eff}/Ni: 2.94 μ_B (solid, 298 K) and 3.20 μ_B (in MeCN, 298 K). Diffraction quality single crystals containing a molecule of MeCN as a solvent of crystallization (**1**·MeCN) were grown by diffusion of diethyl ether into a MeCN solution of the complex.

Preparation of [{(L)Cu(μ-L′)}$_2$][ClO$_4$]$_2$ (2): To a stirred solution of L (0.050 g, 0.212 mmol) in MeOH (3 cm^3) $[Cu(H_2O)_6][ClO_4]_2$ (0.079 g, 0.212 mmol) was added in small portions. After stirring for 30 min, HL′ (0.031 g, 0.212 mmol) was added and the resulting mixture was refluxed for one and half hour. Addition of Et_3N (0.021 g, 0.212 mmol) led to the precipitation of a bluish green microcrystalline solid. It was filtered, washed with a minimum amount of MeOH and dried in vacuo. Recrystallization was achieved by diffusion of diethyl ether (5 cm^3) into a MeCN solution (3 cm^3) of the complex (yield: 0.052 g, ca. 45%). $C_{44}H_{36}Cl_2Cu_2N_{14}O_8$ (1086.84): calcd. C 48.62, H 3.34, N 18.04%; found C 48.95, H 3.41, N 17.83%. Molar conductance, Λ_M (MeCN, 298 K) = 226 Ω^{-1}cm^{2}mol^{-1}. UV/Vis (MeCN), λ_{max}/nm (ε/M^{-1}cm^{-1}): 770 (sh) (70), 640 (120), 300 (sh) (19 400), 290 (sh) (22 700), 253 (46 550). μ_{eff}/Cu: 1.58 μ_B (solid, 299 K) and 1.40 μ_B (in MeCN, 298 K). Diffraction quality single crystals containing two molecules of MeCN as solvent of crystallization (**2**·2MeCN) were grown by diffusion of diethyl ether into a MeCN solution of the complex.

Caution: *Perchlorate salts of compounds containing organic ligands are potentially explosive!*

Physical Measurements: Elemental analyses (C, H, N) were obtained at the Microanalytical Laboratory at this Department. Infrared spectra were recorded on a Bruker Vector 22 spectrophotometer using KBr discs. Electronic spectra were recorded using Agilent 8453 diode-array spectrophotometer. ^{1}H NMR spectral measurements were performed on a Bruker WP 80 (80 MHz) NMR spectrometer. Solution electrical conductivity measurements (298 K) were carried out with an Elico (Hyderabad, India) Type CM-82 T conductivity bridge. X-band EPR were obtained on a Bruker EMX 1444 EPR spectrometer operating at 9.455 GHz (fitted with a quartz Dewar for measurements at 120 K). The spectra were calibrated with diphenylpicrylhydrazyl, DPPH (g = 2.0037).

Magnetism: Magnetic susceptibility measurements on polycrystalline sample of **1** were performed in the temperature range of 2–298 K with a Quantum Design SQUID magnetometer [(Model MPMSXL-5) Valencia, Spain]. For **2** variable temperature magnetic susceptibility measurements in the range 5–300 K was obtained in the solid state using a Quantum Design (Model MPMSXL-5) SQUID (Kanpur, India) magnetic susceptometer operating at a magnetic field of 0.5 T. Magnetic susceptibility measurements in MeCN solution were obtained by Evans's method[42] using a PMX-60 JEOL (60 MHz) NMR spectrometer. Susceptibilities were corrected for diamagnetic contributions, by using literature values.[32] Effective magnetic moments were calculated from $\mu_{eff} = 2.828\,[\chi_M T]^{1/2}$, where χ_M is the corrected molar susceptibility.

Cyclic Voltammetry: Cyclic voltammograms were recorded at 298 K on PAR model 370 electrochemistry system consisting of model 174A polarographic analyzer and model 175 universal programmer. A standard three-electrode cell was employed with a Beckman M-39273 platinum-inlay working electrode, a platinum-wire auxiliary electrode and a saturated calomel electrode (SCE) as reference; no correction was made for junction potentials.

Crystallography: For complex **1**·MeCN diffracted intensities were collected on a Bruker SMART APEX CCD diffractometer, with graphite-monochromated Mo-K_α (λ = 0.71073 Å) radiation at 100(2) K. For data reduction 'Bruker Saint Plus' program was used. Data for **2**·2MeCN were collected at 293 K on a Enraf Nonius MACH2 diffractometer, equipped with graphite-monochromated Mo-K_α radiation (λ = 0.71073 Å). Data were corrected for absorption and the Lorentz and polarization effects. The structures were solved with SIR-92 and refined with the SHELXL-97 package incorporated in WinGX 1.64 crystallographic collective package.[43] Anisotropic refinements were performed by full-matrix least-squares procedure on F^2. The positions of the hydrogen atoms were calculated assuming ideal geometries, but not refined. The data-set of **1**·MeCN was treated with the SQUEEZE filter of PLATON[44] due to the presence of severely disordered solvent molecule(s) (probably acetonitrile, water) which could not be modeled satisfactorily. PLATON estimated the electron count to be 15 electron/cell in a volume of 398.0 Å^3 out of a unit volume of 4307.0 Å^3 (9.2%). Pertinent crystallographic parameters are summarized in Table 3. Intermolecular contacts of the C–H···π and π···π stacking were examined with the DIAMOND package.[45] C–H distances were normalized along the same vectors to the neutron derived values of 1.083 Å.[46]

CCDC-632189 (for **1**·MeCN) and -240140 (for **2**·2MeCN) contain the supplementary crystallographic data for this paper. These data can be obtained free of charge from The Cambridge Crystallographic Data Centre via www.ccdc.cam.ac.uk/data_request/cif.

Supporting Information (see also the footnote on the first page of this article): Figure S1 presents the intermolecular π-π stacking leading to the formation of staircase-like arrangement of molecules

Table 3. Data collection and structure refinement parameters for **1**·MeCN and **2**·2MeCN.

	1·MeCN	**2**·2MeCN
Molecular formula	$C_{46}H_{39}Cl_2Ni_2N_{15}O_8$	$C_{48}H_{42}Cl_2Cu_2N_{16}O_8$
M_r	1118.24	1168.96
Temperature /K	100(2)	293(2)
Radiation used (λ /Å)	Mo-K_α (0.71073)	Mo-K_α (0.71073)
Crystal system	triclinic	triclinic
Space group	$P\bar{1}$ (no. 2)	$P\bar{1}$ (no. 2)
a /Å	12.6720(12)	10.630(9)
b /Å	15.1890(14)	11.689(2)
c /Å	16.1269(15)	12.510(4)
α /°	69.082(2)	109.78(2)
β /°	83.528(2)	102.64(5)
γ /°	69.395(2)	110.46(3)
V /Å	2713.7(4)	1266.3(12)
Z	2	1
D_c /g cm^{-3}	1.369	1.533
μ /mm^{-1}	0.855	1.016
Crystal size /mm	0.20 × 0.10 × 0.10	0.20 × 0.10 × 0.10
Unique reflections, R_{int}	12895, 0.0328	3315, 0.0329
Observed reflections [$I > 2\sigma(I)$]	6959	2457
Refined parameters	662	344
$R^{[a]}(R_w)^{[b]}$	0.0767 (0.1837)	0.0768 (0.2208)
$R^{[a]}(R_w)^{[b]}$ (all data)	0.1364 (0.2068)	0.1182 (0.2407)
Goodness-of-fit on F^2	0.950	1.050

[a] $R(F) = \Sigma(||F_o| - |F_c||)/\Sigma|F_o|$. [b] $R_w(F^2) = \{\Sigma[w(|F_o|^2 - |F_c|^2)^2]/\Sigma[w(|F_o|^2)^2]\}^{1/2}$.

in complex **2**·2MeCN. Figure S2 shows absorption spectral features for both complexes in MeCN. Figure S3 shows the EPR spectra of complex **2** at 293 K and Figure S4 the CV response of electrochemically generated green solution from complex **1**. Figure S5 deals with the CV response of complex **2**.

Acknowledgments

Financial assistance received from the Department of Science and Technology (DST) and the Council of Scientific & Industrial Research (CSIR), Government of India is gratefully acknowledged. We acknowledge the National Single Crystal Diffractometer Facility at the Department of Chemistry, Indian Institute of Technology Kanpur, for data collection of **1**·MeCN. We acknowledge Prof. M. S. Hundal and Dr. G. Hundal (Guru Nanak Dev University, Amritsar, India) for data collection of **2**·2MeCN. We sincerely thank Dr. Jhumpa Mukherjee for variable-temperature magnetic data analysis of complex **2** and Mr. Haritosh Mishra for analysis of noncovalent interactions in the crystal structures. Comments of the reviewers at the revision stage were very helpful.

[1] a) H. van Crawford, H. W. Richardson, J. R. Wasson, D. J. Hodgson, W. E. Hatfield, *Inorg. Chem.* **1976**, *15*, 2107–2110; b) O. Kahn, *Angew. Chem. Int. Ed. Engl.* **1985**, *24*, 834–850; c) T. Kawata, M. Yamanaka, S. Ohba, Y. Nishida, M. Nagamatsu, T. Tokii, M. Kato, O. W. Steward, *Bull. Chem. Soc. Jpn.* **1992**, *65*, 2739–2747; d) S. Meenakumari, S. K. Tiwari, A. R. Chakravarty, *J. Chem. Soc., Dalton Trans.* **1993**, 2175–2181; e) L. K. Thompson, S. K. Mandal, S. K. Tandon, J. N. Bridson, M. K. Park, *Inorg. Chem.* **1996**, *35*, 3117–3125.

[2] a) R. Mukherjee, *Coord. Chem. Rev.* **2000**, *203*, 151–218; b) R. Mukherjee, in *Comprehensive Coordination Chemistry-II: From Biology to Nanotechnology*, Vol. 6 (Eds.: J. A. McCleverty, T. J. Meyer; Volume Ed.: D. E. Fenton), Chapter on Copper, Elsevier/Pergamon, Amsterdam, **2004**, pp. 747–910.

[3] R. Gupta, R. Hotchandani, R. Mukherjee, *Polyhedron* **2000**, *19*, 1429–1435.

[4] J. Mukherjee, R. Mukherjee, *Dalton Trans.* **2006**, 1611–1621.

[5] J. Mukherjee, R. Gupta, T. Mallah, R. Mukherjee, *Inorg. Chim. Acta* **2005**, *358*, 2711–2717.

[6] V. Mishra, F. Lloret, R. Mukherjee, *Inorg. Chim. Acta* **2006**, *359*, 4053–4062.

[7] R. Gupta, R. Mukherjee, *Polyhedron* **2000**, *19*, 719–724.

[8] a) D. Ghosh, T. K. Lal, S. Ghosh, R. Mukherjee, *Chem. Commun.* **1996**, 13–14; b) D. Ghosh, R. Mukherjee, *Inorg. Chem.* **1998**, *37*, 6597–6605.

[9] A. K. Patra, M. Ray, R. Mukherjee, *Polyhedron* **2000**, *19*, 1423–1428.

[10] a) S. Mahapatra, N. Gupta, R. Mukherjee, *J. Chem. Soc., Dalton Trans.* **1992**, 3041–3045; b) J. Mukherjee, V. Balamurugan, R. Gupta, R. Mukherjee, *Dalton Trans.* **2003**, 3686–3692.

[11] a) S. Mahapatra, P. Das, R. Mukherjee, *J. Chem. Soc., Dalton Trans.* **1993**, 217–220; b) T. K. Lal, R. Mukherjee, *Inorg. Chem.* **1998**, *37*, 2373–2382 and references cited therein.

[12] S. P. Foxon, D. Utz, J. Astner, S. Schindler, F. Thaler, F. W. Heinemann, G. Liehr, J. Mukherjee, V. Balamurugan, D. Ghosh, R. Mukherjee, *Dalton Trans.* **2004**, 2321–2328.

[13] S. Mandal, R. Mukherjee, *Inorg. Chim. Acta* **2006**, *359*, 4019–4026.

[14] R. Gupta, S. Mukherjee, R. Mukherjee, *J. Chem. Soc., Dalton Trans.* **1999**, 4025–4030.

[15] a) S. Trofimenko, *Prog. Inorg. Chem.* **1986**, *34*, 115–210; b) G. La Monica, G. A. Ardizzoia, *Prog. Inorg. Chem.* **1997**, *46*, 151–238; c) J. Vela, S. Vaddadi, S. Kingsley, C. J. Flaschenriem, R. J. Lachicotte, T. R. Cundari, P. L. Holland, *Angew. Chem. Int. Ed.* **2006**, *45*, 1607–1611.

[16] M. D. Ward, J. A. McCleverty, J. C. Jeffery, *Coord. Chem. Rev.* **2001**, *222*, 251–272.

[17] a) R. L. Paul, S. M. Couchman, J. C. Jeffery, J. A. McCleverty, Z. R. Reeves, M. D. Ward, *J. Chem. Soc., Dalton Trans.* **2000**, 845–851; b) D. A. McMorran, P. J. Steel, *Chem. Commun.* **2002**, 2120–2121; c) D. A. McMorran, P. J. Steel, *Inorg. Chem. Commun.* **2003**, *6*, 43–47; d) R. L. Paul, Z. R. Bell, J. C. Jeffery, L. P. Harding, J. McCleverty, M. D. Ward, *Polyhedron* **2003**, *22*, 781–787; e) B. A. Leita, B. Moubaraki, K. S. Murray, J. P. Smith, J. D. Cashion, *Chem. Commun.* **2004**, 156–157; f) S. P. Argent, H. Adams, L. P. Harding, T. Riis-Johannessen, J. C. Jefferey, M. D. Ward, *New J. Chem.* **2005**, *29*, 904–911; g) T. K. Ronson, H. Adams, M. D. Ward, *Eur. J. Inorg. Chem.* **2005**, 4533–4549; h) S. P. Argent, H. Adams, T. Riis-Johannessen, J. C. Jefferey, L. P. Harding, W. Clegg, R. W. Harrington, M. D. Ward, *Dalton Trans.* **2006**, 4996–5013.

[18] a) R. Gupta, R. Mukherjee, *Polyhedron* **2001**, *20*, 2545–2549; b) S. Mahapatra, R. J. Butcher, R. Mukherjee, *Indian J. Chem.* **2001**, *40A*, 973–975; c) R. Gupta, T. K. Lal, R. Mukherjee, *Polyhedron* **2002**, *21*, 1245–1253; d) S. Singh, V. Mishra, J. Mukherjee, N. Seethalekshmi, R. Mukherjee, *Dalton Trans.* **2003**, 3392–3397; e) C. Enachescu, J. Linares, F. Varret, K. E. Codjovi, S. G. Salunke, R. Mukherjee, *Inorg. Chem.* **2004**, *43*, 4880–4888; f) H. Mishra, R. Mukherjee, *J. Organomet. Chem.* **2006**, *691*, 3545–3555.

[19] a) V. Balamurugan, M. S. Hundal, R. Mukherjee, *Chem. Eur. J.* **2004**, *10*, 1683–1690; b) V. Balamurugan, W. Jacob, J. Mukherjee, R. Mukherjee, *CrystEngComm* **2004**, *6*, 396–400; c) V. Balamurugan, R. Mukherjee, *CrystEngComm* **2005**, *7*, 337–341; d) V. Balamurugan, R. Mukherjee, *Inorg. Chim. Acta* **2006**, *359*, 1376–1382.

[20] A. J. Amoroso, A. M. C. Thompson, J. C. Jeffery, P. L. Jones, J. A. McCleverty, M. D. Ward, *J. Chem. Soc., Chem. Commun.* **1994**, 2751–2752.

[21] T.-L. Hu, J.-R. Li, C.-S. Liu, X.-S. Shi, J.-N. Zhou, X.-H. Bu, J. Ribas, *Inorg. Chem.* **2006**, *45*, 162–173 and references cited therein.

[22] B. J. Hathaway, in *Comprehensive Coordination Chemistry* (Eds.: G. Wilkinson, R. D. Gillard, J. A. McCleverty), Pergamon, Oxford, **1987**, vol. *5*, pp. 533–774.
[23] W. J. Geary, *Coord. Chem. Rev.* **1971**, *7*, 81–122.
[24] J. Casabó, J. Pons, K. S. Siddiqi, F. Teixidor, E. Molins, C. Miravitlles, *J. Chem. Soc., Dalton Trans.* **1989**, 1401–1403.
[25] a) F. Meyer, E. Kaifer, P. Kircher, K. Heinze, H. Pritzkow, *Chem. Eur. J.* **1999**, *5*, 1617–1630; b) L. Siegfried, T. A. Kaden, F. Meyer, P. Kircher, H. Pritzkow, *J. Chem. Soc., Dalton Trans.* **2001**, 2310–2315; c) J. C. Röder, F. Meyer, E. Kaifer, H. Pritzkow, *Eur. J. Inorg. Chem.* **2004**, *10*, 1646–1660 and references cited therein.
[26] A. W. Addison, T. N. Rao, J. Reedijk, J. van Rijn, G. C. Verschoor, *J. Chem. Soc., Dalton Trans.* **1984**, 1349–1356 (square pyramidal geometry $\tau = 0$; trigonal bipyramidal geometry $\tau = 1$).
[27] S. Tanase, I. A. Koval, E. Bouwman, R. de Gelder, J. Reedijk, *Inorg. Chem.* **2005**, *44*, 7860–7865.
[28] a) T. Kamiusuki, H. Ōkawa, N. Matsumoto, S. Kida, *J. Chem. Soc., Dalton Trans.* **1990**, 195–198; b) T. Kamiusuki, H. Ōkawa, K. Inoue, N. Matsumoto, M. Kodera, S. Kida, *J. Coord. Chem.* **1991**, *23*, 201–211; c) F. Degang, W. Guoxiong, Z. Zongyuan, Z. Xiangge, *Transition Met. Chem.* **1994**, *19*, 592–594; d) E. Spodine, A. M. Atria, J. Valenzuela, J. Jalocha, J. Manzur, A. M. García, M. T. Garland, O. Peña, J.-Y. Saillard, *J. Chem. Soc., Dalton Trans.* **1999**, 3029–3034; e) L. Lamarque, P. Navarro, C. Miranda, V. J. Arán, C. Ochoa, F. Escartí, E. García-España, J. Latorre, S. V. Luis, J. F. Miravet, *J. Am. Chem. Soc.* **2001**, *123*, 10560–10570; f) M. J. Hallam, C. A. Kilner, M. A. Halcrow, *Acta Crystallogr., Sect. C* **2002**, *58*, m445–m446.
[29] a) M. Munakata, L. P. Wu, M. Yamamoto, T. Kuroda-Sowa, M. Maekawa, S. Kawata, S. Kitagawa, *J. Chem. Soc., Dalton Trans.* **1995**, 4099–4103; b) C. Miranda, F. Escartí, L. Lamarque, E. García-España, P. Navarro, J. Latorre, F. Lloret, H. R. Jiménez, M. J. R. Yunta, *Eur. J. Inorg. Chem.* **2005**, 189–208.
[30] a) D. L. Reger, J. R. Gardinier, R. F. Semeniuc, M. D. Smith, *Dalton Trans.* **2003**, 1712–1718; b) D. L. Reger, R. F. Semeniuc, M. D. Smith, *Cryst. Growth Des.* **2005**, *5*, 1181–1190; c) C. Janiak, *J. Chem. Soc., Dalton Trans.* **2000**, 3885–3896.
[31] F. A. Cotton, G. Wilkinson, C. A. Murillo, M. Bochmann, *Advanced Inorganic Chemistry*, Wiley, New York, 6th ed., **1999**.
[32] G. De Munno, M. Julve, F. Lloret, A. Derory, *J. Chem. Soc., Dalton Trans.* **1993**, 1179–1184.
[33] E. Aznar, S. Ferrer, J. Borrás, F. Lloret, M. Liu-González, H. Rodríguez-Prieto, S. García-Granda, *Eur. J. Inorg. Chem.* **2006**, 5115–5125.
[34] F. Lloret, J. Sletten, R. Ruiz, M. Julve, J. Faus, M. Verdaguer, *Inorg. Chem.* **1992**, *31*, 778–784.
[35] I. Castro, J. Sletten, M. L. Calatayud, M. Julve, J. Cano, F. Lloret, A. Caneschi, *Inorg. Chem.* **1995**, *34*, 4903–4909.
[36] O. Kahn, *Molecular Magnetism,* VCH Publishers, New York, **1993**.
[37] R. Ruiz, F. Lloret, M. Julve, M. C. Muñoz, C. Bois, *Inorg. Chim. Acta* **1994**, *219*, 179–186.
[38] R. Ruiz, F. Lloret, M. Julve, J. Faus, M. C. Muñoz, X. Solans, *Inorg. Chim. Acta* **1993**, *213*, 261–268.
[39] a) T. R. Holman, M. P. Hendrich, L. Que Jr, *Inorg. Chem.* **1992**, *31*, 937–939; b) B. Kersting, D. Siebert, *Inorg. Chem.* **1998**, *37*, 3820–3828.
[40] a) F. Meyer, H. Kozlowski, *Comprehensive Coordination Chemistry* II: *From Biology to Nanotechnology*, Pergamon, **2004**, *6*, 247–554; b) K. Nag, A. Chakravorty, *Coord. Chem. Rev.* **1980**, *33*, 87–147; c) R. I. Haines, A. McAuley, *Coord. Chem. Rev.* **1981**, *39*, 77–119; d) A. G. Lappin, A. McAuley, *Adv. Inorg. Chem.* **1988**, *32*, 241–295.
[41] A. K. Patra, R. Mukherjee, *Inorg. Chem.* **1999**, *38*, 1388–1393.
[42] D. F. Evans, *J. Chem. Soc.* **1959**, 2003–2004.
[43] L. J. Farrugia, *WinGX ver. 1.64*, An Integrated Systems of Windows Programs for the Solution, Refinement and Analysis of Single-Crystal X-ray Diffraction Data, Department of Chemistry, University of Glasgow, **2003**.
[44] PLATON: A. L. Spek, *J. Appl. Crystallogr.* **2003**, *36*, 7–13.
[45] *DIAMOND ver 2.1c*, Crystal Impact GbR, Bonn, Germany, **1999**.
[46] T. Steiner, *Angew. Chem. Int. Ed.* **2002**, *41*, 48–76.

Received: January 3, 2007
Published Online: April 4, 2007

